Monthly Notices of the ROYAL ASTRONOMICAL SOCIETY

MNRAS 472, 3971–3978 (2017) doi:10.1093/mnras/stx2204
Advance Access publication 2017 August 26

On the internal structure of relativistic jets collimated by ambient gas pressure

V. S. Beskin,[1,2★] A. V. Chernoglazov,[1★] A. M. Kiselev[1,2] and E. E. Nokhrina[1]

[1]Moscow Institute of Physics and Technology, Dolgoprudny, Institutsky per. 9, Moscow 141700, Russia
[2]P. N. Lebedev Physical Institute, Leninsky prosp. 53, Moscow 119991, Russia

Accepted 2017 August 22. Received 2017 August 17; in original form 2017 July 18

ABSTRACT

Recent progress in very long baseline interferometry (VLBI) observations of relativistic jets outflowing from active galactic nuclei gives us direct information about jet width $r_{\rm jet}(l)$ dependence on the distance l from the 'central engine'. Being the missing link in previous works, this relation opens the possibility of determining the internal structure of a jet. In this article, we consider a relativistic jet submerged in an external medium with finite gas pressure $P_{\rm ext}$. Neither an external magnetic field nor an infinitely thin current sheet will be assumed. This approach allows us to construct a reasonable solution in which both the magnetic field and the flow velocity vanish at the jet boundary $r = r_{\rm jet}$. In particular, the connection between external gas pressure and internal structure of a relativistic jet is determined.

Key words: galaxies: active – galaxies: jets.

1 INTRODUCTION

The most visible activity in compact astrophysical sources is connected with strongly collimated jets. They are observed both in relativistic objects such as active galactic nuclei (AGNs) and microquasars and in young stars where the motion of matter is non-relativistic. Definite progress in recent very long baseline interferometry (VLBI) observations of relativistic jets outflowing from active galactic nuclei (Lobanov 1998a; Cohen et al. 2007; Clausen-Brown et al. 2013; Kardashev et al. 2014) gives us new information concerning their physical characteristics and dynamics.

According to the commonly accepted point of view, the nature of relativistic jets from AGNs is associated with highly magnetized magnetohydrodynamical (MHD) flow originating due to fast rotation of supermassive black holes (Blandford 1976; Lovelace 1976; Krolik 1999; Beskin 2009; Meier 2012). Within this approach, it is believed that electromagnetic energy flux plays the main role in energy transfer from the 'central engine' to active regions. The poloidal magnetic field generated in the disc links the rotating 'central engine' (the disc and the black hole) and infinity. Thus, plasma outflow and energy flux propagate along magnetic field lines. Due to differential rotation of the disc and gas inertness, the field lines are twisted, a toroidal component of the field occurs and the field pressure connected with this component can collimate the gas.

More than 40 years of very extensive analytical (Heyvaerts & Norman 1989; Pelletier & Pudritz 1992; Lery, Heyvaerts & Appl 1998; Tomimatsu & Takahashi 2003; Beskin & Malyshkin 2000; Komissarov et al. 2007; Zakamska, Begelman & Blandford 2008; Beskin 2009; Lyubarsky 2009) and numerical (Koide, Shibata & Kudoh 1999; Gracia et al. 2009; Komissarov et al. 2009; Tchekhovskoy, McKinney & Narayan 2009; Porth et al. 2011; Mizuno et al. 2012; McKinney, Tchekhovskoy & Blandford 2012; Penna, Narayan & Sądowski 2013; Tchekhovskoy & Bromberg 2016; Mościbrodzka, Falcke & Shiokawa 2016) explorations allow us to clarify a number of very important features of relativistic jets. In particular, it was demonstrated both analytically (Beskin & Nokhrina 2006) and numerically (McKinney 2006; Komissarov et al. 2009; Tchekhovskoy et al. 2009; Porth et al. 2011) that, for highly elongated relativistic jets, very effective bulk acceleration can take place. Remember that, in the quasi-spherical case, the flow remains magnetically dominated (Tomimatsu 1994; Beskin, Kuznetsova & Rafikov 1998). Numerical simulations show that the MHD model can also explain jet collimation. For this reason, the MHD model remains the most reliable in the context of the problem of the origin and stability of jets and an explanation for the energetics of the central black hole.

On the other hand, some key points remain unclear up to now. In many articles dealing with the MHD model of these objects, in which jet formation was connected with the attraction of longitudinal currents flowing in the magnetosphere, the majority of attention was given to proper collimation, in the sense that the environment was supposed to be of no importance (Blandford & Payne 1982; Heyvaerts & Norman 1989; Pelletier & Pudritz 1992; Sulkanen & Lovelace 1990; Li, Chiueh & Begelman 1992; Sauty & Tsinganos 1994). However, as was shown later, this is possible only for non-zero total current I flowing within a jet and the problem is to close it in the outer regions of the magnetosphere.

Moreover, it is quite clear that the collimation problem cannot be solved while ignoring the environment (see e.g. Appl & Camenzind 1992, 1993). In particular, this is already evident from

★ E-mail: beskin@lpi.ru (VSB); alexander.chernoglazov@gmail.com (AVC)

© 2017 The Authors
Published by Oxford University Press on behalf of the Royal Astronomical Society

Downloaded from https://academic.oup.com/mnras/article-abstract/472/4/3971/4094905/On-the-internal-structure-of-relativistic-jets
by MPI Study of Societies user
on 10 October 2017

the example of the magnetosphere of a compact object with a monopole magnetic field, since, for any arbitrarily small external regular magnetic field, the monopole solution (for which the poloidal magnetic field decreases as r^{-2}) cannot be extended to infinity. Moreover, as is well-known from the example of moving space bodies such as Jupiter's satellites (Zheleznyakov 1996) or artificial Earth satellites (Al'pert, Gurevich & Pitaevskii 1965), the external magnetic field can serve as an efficient transmission chain, sometimes defining the total energy losses in the system.

Thus, one of the most important questions concerns the flow structure nearby the jet boundary in the current closure region. In general, the necessity to close the electric current in the cocoon region (for both AGNs and young stellar objects) was recognized many years ago (Lesch, Appl & Camenzind 1989; Benford & Protheroe 2008b). However, the very topology of the magnetic field in this domain remains unknown. Most researchers consider a quasi-homogeneous longitudinal magnetic field but, according to another point of view, ascending to the idea of the 'magnetic tower' (Lynden-Bell 1996, 2003), a longitudinal magnetic field can change direction in the vicinity of the jet boundary (Lico et al. 2007; Benford & Protheroe 2008a; Kim et al. 2016, 2017).

Another point is connected with the question of whether there is a contact discontinuity on the jet boundary or whether all values go over smoothly into the external environment. In most articles, an infinitely thin current sheet was actually introduced (Lery et al. 1998; Beskin & Malyshkin 2000; Lyubarsky 2009; Beskin & Nokhrina 2010), the internal structure of which has not been described carefully enough. The difficulty is connected with a very low energy density of the external media in comparison with one inside the relativistic jet. For this reason, in some articles the external media were modelled by a homogeneous magnetic field with energy density $B_{\rm ext}^2/8\pi = P_{\rm ext}$.

In this article, we present an approach that is free of the difficulties mentioned above. In other words, we consider a relativistic jet submerged in an external medium with finite gas pressure $P_{\rm ext}$. Neither an external magnetic field nor an infinitely thin current sheet will be assumed. The main new point connects with the boundary conditions. In what follows, we assume that both the magnetic field and the flow velocity vanish at the jet boundary $r = r_{\rm jet}$. On the other hand, we suppose that the flow remains supersonic. It is shown that this approach allows us not only to construct a reasonable solution but also to determine the connection between the external gas pressure and internal structure of a relativistic jet.

2 GRAD–SHAFRANOV APPROACH FOR CYLINDRICAL FLOW

2.1 Basic equations

In this section we recall the main relations of the Grad–Shafranov approach. The basic equations describing the internal structure of relativistic and non-relativistic jets within this approach were formulated about 30 years ago (Heyvaerts & Norman 1989; Pelletier & Pudritz 1992; Lery et al. 1998). This method allows us to determine the internal structure of cylindrical jets, knowing in the general case five 'integrals of motion', i.e. energy $E(\Psi)$ and angular momentum $L(\Psi)$ flux, electric potential, which connects with angular velocity $\Omega_{\rm F}(\Psi)$, entropy $s(\Psi)$ and particle-to-magnetic flux ratio $\eta(\Psi)$. All these values are to be constant along magnetic surfaces: $\Psi = $ const.

As has been shown by Beskin & Nokhrina (2006), a one-dimensional (1D) cylindrical approximation describes well enough the internal structure of parabolic jets starting from sufficiently small distances from the 'central engine' corresponding to a fast magnetosonic surface ($l_{\rm F} \sim 0.01$ pc for ordinary AGNs). It allows us to discuss parsec-scale jets within a much more simple cylindrical geometry.

As a result, for cylindrical flows we can write the electric $\boldsymbol{E}$ and magnetic $\boldsymbol{B}$ fields, as well as the four-velocity of a plasma $\boldsymbol{u} = \gamma \boldsymbol{v}/c$, as

$$\boldsymbol{B} = \frac{1}{2\pi r}\frac{{\rm d}\Psi}{{\rm d}r}\boldsymbol{e}_z - \frac{2I}{rc}\boldsymbol{e}_\varphi, \tag{1}$$

$$\boldsymbol{E} = -\frac{\Omega_{\rm F}}{2\pi c}\frac{{\rm d}\Psi}{{\rm d}r}\boldsymbol{e}_r, \tag{2}$$

$$\boldsymbol{u} = \frac{\eta}{n}\boldsymbol{B} + \gamma\left(\frac{\Omega_{\rm F} r}{c}\right)\boldsymbol{e}_\varphi. \tag{3}$$

Here $\Psi(r)$ is the flux function, i.e. the flux of magnetic field through the circle with radius r:

$$\Psi(r) = 2\pi\int_0^r B_z(r')\, r'\, {\rm d}r' \tag{4}$$

and I is the total electric current through this circle. Finally, n is the number density in the comoving reference frame and $\gamma^2 = \boldsymbol{u}^2 + 1$ is the hydrodynamical Lorentz factor.

In addition to integrals $\Omega_{\rm F}(\Psi)$ and $\eta(\Psi)$ determining the electromagnetic fields and hydrodynamical four-velocity, the total energy flux $E(\Psi)$ and z-component of the angular momentum flux $L(\Psi)$,

$$E(\Psi) = \gamma\mu\eta + \frac{\Omega_{\rm F} I}{2\pi}, \tag{5}$$

$$L(\Psi) = \frac{r u_\varphi \mu\eta}{c} + \frac{I}{2\pi}, \tag{6}$$

are to be determined from the boundary and critical conditions. Accordingly, the trans-field Grad–Shafranov equation can be rewritten as (see e.g. Beskin 2009)

$$\frac{1}{r}\frac{\rm d}{{\rm d}r}\left(\frac{A}{r}\frac{{\rm d}\Psi}{{\rm d}r}\right) + \frac{\Omega_{\rm F}}{c^2}\left(\frac{{\rm d}\Psi}{{\rm d}r}\right)^2\frac{{\rm d}\Omega_{\rm F}}{{\rm d}\Psi} + \frac{32\pi^4}{r^2\mathcal{M}^2}\frac{\rm d}{{\rm d}\Psi}\left(\frac{G}{A}\right)$$
$$- \frac{64\pi^4\mu^2}{\mathcal{M}^2}\eta\frac{{\rm d}\eta}{{\rm d}\Psi} - 16\pi^3 nT\frac{{\rm d}s}{{\rm d}\Psi} = 0, \tag{7}$$

where

$$G = r^2(E - \Omega_{\rm F} L)^2 + \mathcal{M}^2 L^2 c^2 - \mathcal{M}^2 r^2 E^2. \tag{8}$$

Here, T is the temperature,

$$A = 1 - \Omega_{\rm F}^2 r^2/c^2 - \mathcal{M}^2 \tag{9}$$

is the Alfvénic factor,

$$\mathcal{M}^2 = \frac{4\pi\mu\eta^2}{n} \tag{10}$$

is the Alfvénic Mach number,

$$\mu = m_{\rm p}c^2 + m_{\rm p}w \tag{11}$$

is the relativistic enthalpy (w is non-relativistic enthalpy) and the derivative ${\rm d}/{\rm d}\Psi$ acts on the integrals of motion only. Finally, the relativistic Bernoulli equation $u_{\rm p}^2 = \gamma^2 - u_\varphi^2 - 1$ has the form

$$\frac{\mathcal{M}^4}{64\pi^4 r^2}\left(\frac{{\rm d}\Psi}{{\rm d}r}\right)^2 = \frac{K}{r^2 A^2} - \mu^2\eta^2, \tag{12}$$

Downloaded from https://academic.oup.com/mnras/article-abstract/472/4/3971/4094905/On-the-internal-structure-of-relativistic-jets
by MPI Study of Societies user
on 10 October 2017

where

$$K = r^2(e')^2(A - \mathcal{M}^2) + \mathcal{M}^4 r^2 E^2 - \mathcal{M}^4 L^2 c^2 \tag{13}$$

and $e' = E - \Omega_F L$.

As was shown by Beskin & Malyshkin (2000), it is convenient for cylindrical flow to reduce one second-order Grad–Shafranov equation to two first-order ordinary differential equations for magnetic flux $\Psi(r)$ and poloidal Alfvénic Mach number $\mathcal{M}(r)$. Multiplying equation (7) by $2A\,\mathrm{d}\Psi/\mathrm{d}r$ and using equation (12), one can obtain, for the general case taking thermal effects into consideration (Beskin & Nokhrina 2006),

$$\left[\frac{(e')^2}{\mu^2\eta^2} - 1 + \frac{\Omega_F^2 r^2}{c^2} - A\frac{c_s^2}{c^2}\right]\frac{\mathrm{d}\mathcal{M}^2}{\mathrm{d}r} = \frac{\mathcal{M}^6 L^2 c^2}{A r^3 \mu^2 \eta^2}$$
$$+ \frac{\Omega_F^2 r \mathcal{M}^2}{c^2}\left[2 - \frac{(e')^2}{A\mu^2\eta^2}\right] + \mathcal{M}^2 \frac{e'}{\mu^2\eta^2}\frac{\mathrm{d}\Psi}{\mathrm{d}r}\frac{\mathrm{d}e'}{\mathrm{d}\Psi}$$
$$+ \frac{\mathcal{M}^2 r^2}{2c^2}\frac{\mathrm{d}\Psi}{\mathrm{d}r}\frac{\mathrm{d}\Omega_F^2}{\mathrm{d}\Psi} - \mathcal{M}^2\left(1 - \frac{\Omega_F^2 r^2}{c^2} + 2A\frac{c_s^2}{c^2}\right)\frac{\mathrm{d}\Psi}{\mathrm{d}r}\frac{1}{\eta}\frac{\mathrm{d}\eta}{\mathrm{d}\Psi}$$
$$- \left[\frac{A}{n}\left(\frac{\partial P}{\partial s}\right)_n + \left(1 - \frac{\Omega_F^2 r^2}{c^2}\right)T\right]\frac{\mathcal{M}^2}{\mu}\frac{\mathrm{d}\Psi}{\mathrm{d}r}\frac{\mathrm{d}s}{\mathrm{d}\Psi}. \tag{14}$$

Here, c_s is the sound velocity, defined by $c_s^2 = (\mathrm{d}P/\mathrm{d}n)|_s/m_p$ (in what follows we consider the case $c_s \ll c$), m_p is particle mass and P is gas pressure. Together with the Bernoulli equation (12), it forms the system of two ordinary differential equations for the Mach number $\mathcal{M}^2(r)$ and magnetic flux $\Psi(r)$ describing cylindrical relativistic jets.

It is important that, by determining the functions $\mathcal{M}^2(r)$ and $\Psi(r)$, one can find the jet radius $r_{\rm jet}$ as well as the profile of the current $I(r)$, the particle energy and the toroidal component of the four-velocity using standard algebraic expressions:

$$\frac{I}{2\pi} = \frac{L - \Omega_F r^2 E/c^2}{1 - \Omega_F^2 r^2/c^2 - \mathcal{M}^2}, \tag{15}$$

$$\gamma = \frac{1}{\mu\eta c^2}\frac{(E - \Omega_F L) - \mathcal{M}^2 E}{1 - \Omega_F^2 r^2/c^2 - \mathcal{M}^2}, \tag{16}$$

$$u_\varphi = \frac{1}{\mu\eta c r}\frac{(E - \Omega_F L)\Omega_F r^2/c^2 - L\mathcal{M}^2}{1 - \Omega_F^2 r^2/c^2 - \mathcal{M}^2}. \tag{17}$$

Finally, as one can easily check, outside the central core ($r \gg c/\Omega_0$) for super-Alfvénic flow ($\mathcal{M}^2 \gg 1$ and neglecting thermal effects), equation (14) can be rewritten in the simple form (Beskin & Malyshkin 2000)

$$\frac{\mathrm{d}}{\mathrm{d}r}\left(\frac{\Omega_F r^2 \mu\eta}{\mathcal{M}^2}\right) - \frac{\mathcal{M}^2}{\mu\eta\Omega_F r^3(\Omega_F^2 r^2/c^2 + \mathcal{M}^2)}L^2 = 0. \tag{18}$$

Without the last term $\propto L^2(\Psi)$, equation (18) results in the conservation of quantity H,

$$H = \frac{\Omega_F r^2 \mu\eta}{\mathcal{M}^2} = \text{const}, \tag{19}$$

that was found by Heyvaerts & Norman (1989) for a conical magnetic field. On the other hand, comparing this relation with the definition of current I (15), one finds that, for non-relativistic flow on the edge of a jet ($E = \mu\eta$, $\mathcal{M}^2 > \Omega_F^2 r^2/c^2$),

$$H = \frac{I}{2\pi}. \tag{20}$$

2.2 Integrals of motion and boundary conditions

As was already stressed, the system of two first-order ordinary differential equations (12), (14) contains five integrals of motion. In the general case, they are to be specified from boundary conditions at the surface of the 'central engine' and from the critical condition at singular surfaces (see e.g. Beskin 2009 for more detail). On the other hand, for cylindrical flow these integrals are free. For this reason, below we control only the reasonableness of our choice.

First of all, to describe the very boundary of a jet (i.e. the domain of current closure), we have to specify integrals of motion in the region $\Psi \approx \Psi_{\rm tot}$, where $\Psi_{\rm tot}$ is the given total magnetic flux in a jet. As, according to (15), the condition of full closing of the current within the jet $I(\Psi_{\rm tot}) = 0$ can be rewritten as $L(\Psi_{\rm tot}) = 0$ and $\Omega_F(\Psi_{\rm tot}) = 0$, in what follows we use the following expressions for these integrals (cf. Beskin & Nokhrina 2010):

$$L(\Psi) = \frac{\Omega_0 \Psi}{4\pi^2 c^2}\sqrt{1 - \frac{\Psi}{\Psi_{\rm tot}}}, \tag{21}$$

$$\Omega_F(\Psi) = \Omega_0\sqrt{1 - \frac{\Psi}{\Psi_{\rm tot}}}, \tag{22}$$

where Ω_0 is the characteristic angular velocity near the rotation axis. In the vicinity of a rotation axis, these invariants correspond to the well-known analytical force-free solution for a homogeneous poloidal magnetic field. On the other hand, both of them vanish at the jet boundary. This fact guarantees the fulfilment of the condition $I(\Psi_{\rm tot}) = 0$. For linear space diminishing of a magnetic field $B(r) \propto (r_{\rm jet} - r)$, this root dependence on Ψ implies linear diminishing of $L(r)$ and $\Omega_F(r)$ as well. Recall also that this root dependence takes place for a homogeneous magnetic field in the vicinity of the central black hole (Beskin 2009).

As was already stressed, in this article we assume that both the magnetic field $\boldsymbol{B}$ and the flow four-velocity $\boldsymbol{u}$ vanish at the jet boundary $r = r_{\rm jet}$. As one can see from (15) and (17), our choice of $L(\Psi)$ and $\Omega_F(\Psi)$ guarantees that toroidal components B_φ and u_φ vanish at the jet boundary. On the other hand, according to (3), for poloidal components one can write $n\boldsymbol{u}_p = \eta\boldsymbol{B}_p$. Thus, the conditions $\boldsymbol{u}_p = 0$ and $\boldsymbol{B}_p = 0$ can be implemented for finite n and η. For simplicity, we consider the case here:

$$\eta(\Psi) = \eta = \text{const}. \tag{23}$$

Further, below we suppose that the flow remains supersonic up to the very boundary: $\mathcal{M}(r_{\rm jet}) > 1$. This supposition allows us to do our consideration less complex. Indeed, in this case equation (14) has no additional singularity at the Alfvenic surface $A = 0$ in the vicinity of the jet boundary.

As to the energy (Bernoulli) integral $E(\Psi)$, we can write

$$E(\Psi) = \Omega_F L + \mu_0\eta\gamma(\Psi). \tag{24}$$

Here, $\gamma(0) = \gamma_{\rm in}$ is the injection Lorentz factor along the jet axis and $\gamma(\Psi_{\rm tot}) = 1$. The last relation implies that the flow velocity vanishes at the jet boundary. As to relativistic enthalpy $\mu_0 = m_p c^2 + m_p w_0$ (11), we consider it here as a constant with $w_0 = c_0^2/(\Gamma - 1)$, where constant c_0 corresponds to the sonic velocity of a flow at the very boundary.[1] Certainly, relativistic enthalpy μ in equations (12) and

[1] In this article we use a polytropic equation of state with polytropic index Γ.

Downloaded from https://academic.oup.com/mnras/article-abstract/472/4/3971/4094905/On-the-internal-structure-of-relativistic-jets
by MPI Study of Societies user
on 10 October 2017

(14) is to be determined via the local value $w = c_s^2/(\Gamma - 1)$ (see below). Finally, in what follows we put also,

$$s(\Psi) = s = \text{const}. \tag{25}$$

As we will see it is this non-zero value that allows us to match a magnetically dominated flow to an external medium with finite pressure.

In addition to five integrals of motion, the system (12), (14) needs two boundary conditions. The first one is the clear condition at the symmetry axis,

$$\Psi(0) = 0. \tag{26}$$

The second one can be found from the pressure balance $P_{\rm ext} = \Gamma^{-1} c_0^2 m_{\rm p} n_0$, where n_0 is the number density of a flow at the jet boundary. Thus, we can determine the jet radius $r_{\rm jet}$ as a function of $P_{\rm ext}$ self-consistently, as the conditions $\boldsymbol{v}(r_{\rm jet}) = 0$ and $\boldsymbol{B}(r_{\rm jet}) = 0$ are automatically fulfilled at $\Psi = \Psi_{\rm tot}$. Now, using definition (10), one can write the second boundary condition, $\mathcal{M}_0^2 = \mathcal{M}^2(r_{\rm jet})$, as

$$\mathcal{M}_0^2 = \frac{4\pi\Gamma^{-1} m_{\rm p}^2 c^2 c_0^2 \eta^2}{P_{\rm ext}}. \tag{27}$$

It is necessary to note that, according to our supposition, $\mathcal{M}_0^2 > 1$, i.e. c_0^2 cannot be very small to fulfil this assumption. Accordingly, in case $c_s \ll c$ the local non-relativistic enthalpy w looks like

$$w = \frac{c_0^2}{(\Gamma - 1)} \left(\frac{\mathcal{M}_0^2}{\mathcal{M}^2}\right)^{\Gamma - 1} \tag{28}$$

and, accordingly, $\mu = m_{\rm p} c^2 + m_{\rm p} w$. This definition emphasizes the insignificance of thermal effects in the vicinity of the rotation axis and corresponds to the usual non-relativistic enthalpy near to the jet boundary. Thanks to these definitions, the system of equations (12), (14) now becomes fully determined.[2]

Thus, we see that the physical answer depends on one external parameter only, namely on the ambient pressure $P_{\rm ext}$. On the other hand, as the sonic velocity c_0 of a flow is fully determined by our choice of the Bernoulli integral $E(\Psi)$ (24), i.e. it does not coincide with the ambient sonic velocity, the solution inevitably contains a contact discontinuity. However, unlike the electromagnetic discontinuity widely considered thus far, there is a hydrodynamical discontinuity only.

It is convenient to rewrite $\mathcal{M}_0^2$ (27) as

$$\mathcal{M}_0^2 = \frac{1}{2\Gamma\sigma_{\rm M}^2} \frac{c_0^2}{c^2} \frac{B_{\rm L}^2}{8\pi P_{\rm ext}}. \tag{29}$$

Here, by definition,

$$B_{\rm L} = \frac{\Psi_{\rm tot}}{\pi R_{\rm L}^2} \tag{30}$$

is the magnetic field at the light cylinder $R_{\rm L} = c/\Omega_0$. Accordingly,

$$\sigma_{\rm M} = \frac{\Omega_0^2 \Psi_{\rm tot}}{8\pi^2 \mu\eta c^2} \tag{31}$$

is the so-called Michel (1969) magnetization parameter, which is the main dimensionless parameter of the problem under consideration.

Recall that the physical meaning of the Michel magnetization parameter is the maximum Lorentz factor γ of the hydrodynamical flow when all electromagnetic energy flux is transferred to particles. At present, rather small values $\sigma_{\rm M} \sim 10$–10^3 are supposed for real relativistic jets (Lobanov 1998b; Nokhrina et al. 2015), but much larger values are also discussed. For this reason, below we consider $\sigma_{\rm M}$ as a free parameter.

It is necessary to stress out that the magnetization parameter $\sigma_{\rm M}$ (31) introduced above represents its amplitude value. As one can see from equation (6), the maximum Lorentz factor at a given magnetic surface,

$$\gamma_{\rm max} = \frac{E(\Psi)}{\mu\eta}, \tag{32}$$

for our choice of invariants (21), (22) looks like

$$\gamma_{\rm max}(\Psi) = 2\sigma_{\rm M} \frac{\Psi}{\Psi_{\rm tot}} \left(1 - \frac{\Psi}{\Psi_{\rm tot}}\right). \tag{33}$$

Finally, analysing the relations (15)–(17), one finds that, for supersonic flow ($\mathcal{M}^2 \gg 1$), the following conditions,

$$1 \ll x_{\rm jet}^2 \ll \mathcal{M}^2 \sigma_{\rm M}, \tag{34}$$

need to be satisfied. Here and below we the use dimensionless radial coordinate

$$x = \frac{\Omega_0 r}{c}, \tag{35}$$

i.e. the radial distance normalized to the light cylinder $R_{\rm L}$. For parsec-scale relativistic jets, $x_{\rm jet} \sim 10^3$–10^5 (see e.g. Mertens et al. 2016).

3 INTERNAL STRUCTURE OF RELATIVISTIC JETS

3.1 Constructing the solution

In Fig. 1, we show an example of the solution of the system of two ordinary differential equations (12), (14). As we see in the outer region in the vicinity of the jet boundary the Mach number $\mathcal{M}$ abruptly decreases. According to definition (10), this implies that the number density increases outward and hence the gradient of gas pressure for non-zero entropy is directed inward. It is this force that balances the pressure of the magnetic field decreasing toward the jet boundary.

As was already stressed, the main problem that hindered the construction of a self-consistent solution was connected with the very small ambient gas pressure in comparison with the electromagnetic

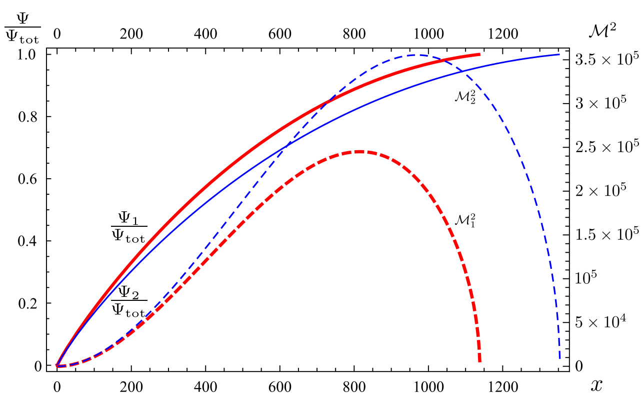

Figure 1. Typical solutions of of the system of two ordinary differential equations (12), (14) for Ψ (solid lines) and $\mathcal{M}^2$ (dashed lines) for $\sigma_{\rm M} = 100$. Thick and thin lines correspond to solutions with boundary Mach number $\mathcal{M}^2(0) = 6400$ and $\mathcal{M}^2(0) = 9100$, respectively. The terminations of these lines are radii of the jet.

[2] This last step was not made by Beskin & Nokhrina (2010).

Downloaded from https://academic.oup.com/mnras/article-abstract/472/4/3971/4094905/On-the-internal-structure-of-relativistic-jets
by MPI Study of Societies user
on 10 October 2017

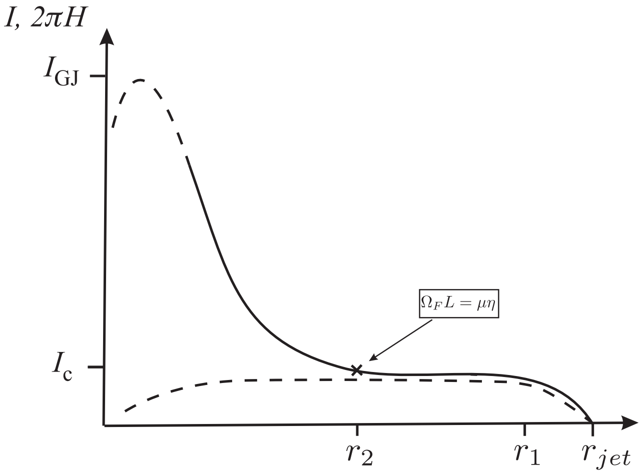

Figure 2. Current close region in the vicinity of a jet boundary (not to scale). The dashed curve corresponds to invariant H (52).

pressure inside a relativistic jet. In our consideration, the current closure follows from our choice of integrals $\Omega_{\rm F}(\Psi)$ and $L(\Psi)$. As a result, return current flows in a wide region corresponding to the domain where $L(\Psi)$ diminishes with Ψ. In this region, the magnetic stress is balanced by the electric one, so that $B_\varphi \approx E_r$. Only near the very boundary of a jet does the gas pressure become important.

As a result, the shooting method (when we vary the Mach number $\mathcal{M}(0)$ at the axis to fulfil the boundary condition $\mathcal{M}(\Psi_{\rm tot}) = \mathcal{M}_0$) meets significant computational difficulties. Simultaneously, this approach says nothing about the structure of the boundary of a jet. For this reason, below we determine the asymptotic behaviour for a $r \to r_{\rm jet}$ moving analytically inwards from radius $r = r_{\rm jet}$. As is shown in Fig. 2, there are two characteristic radii, r_1 and r_2, all of them, as is clear from Fig. 1, located in the close vicinity of the jet boundary. For this reason, in what follows we put $r_1 \approx r_2 \approx r_{\rm jet}$.

3.2 Boundary layer

At first, let us consider the very boundary of a jet $r_1 < r < r_{\rm jet}$. In this region, the leading terms of equation (14) can be written as

$$\left[\frac{\Omega_0^2 r^2}{c^2}\left(1 - \frac{\Psi}{\Psi_{\rm tot}}\right) + \mathcal{M}^2\frac{c_{\rm s}^2}{c^2}\right]\frac{{\rm d}\mathcal{M}^2}{{\rm d}r} = -\frac{\mathcal{M}^4 L^2 c^2}{{}^3\mu^2\eta^2}$$
$$+ 2\frac{\Omega_{\rm F}^2 r\mathcal{M}^2}{c^2} + \mathcal{M}^2\frac{e'}{\mu^2\eta^2}\frac{{\rm d}\Psi}{{\rm d}r}\frac{{\rm d}e'}{{\rm d}\Psi} + \frac{1}{2}\mathcal{M}^2\frac{r^2}{c^2}\frac{{\rm d}\Psi}{{\rm d}r}\frac{{\rm d}\Omega_{\rm F}^2}{{\rm d}\Psi}. \quad (36)$$

As far as Bernoulli equation (12) is concerned, here it is possible to use its non-relativistic version (Heyvaerts & Norman 1989; Beskin 2009):

$$\frac{\mathcal{M}^4}{64\pi^4\eta_{\rm n}^2}\left(\frac{{\rm d}\Psi}{{\rm d}r}\right)^2 = 2r^2(E_{\rm n} - w)$$
$$- \frac{(\Omega_{\rm F}r^2 - L_{\rm n}\mathcal{M}^2)^2}{(1-\mathcal{M}^2)^2} - 2\Omega_{\rm F}r^2\frac{L_{\rm n} - \Omega_{\rm F}r^2}{1-\mathcal{M}^2}. \quad (37)$$

Here,

$$E_{\rm n} = \frac{E}{m_{\rm p}\eta} - c^2 = \frac{\Omega_{\rm F} I}{2\pi c\eta_{\rm n}} + v^2/2 + w \quad (38)$$

is the non-relativistic Bernoulli integral, $w = c_{\rm s}^2/(\Gamma - 1)$ is the non-relativistic enthalpy (again, Γ is the polytropic index), $\eta_{\rm n} = m_{\rm p}c\eta$ and $L_{\rm n} = cL/\eta_{\rm n}$. For a non-relativistic outflow, it is possible to use reduced expressions (Weber & Davis 1967):

$$\frac{I_{\rm n}}{2\pi} = c\eta_{\rm n}\frac{L_{\rm n} - \Omega_{\rm F}r^2}{1-\mathcal{M}^2}, \quad (39)$$

$$v_\varphi = \frac{1}{r}\frac{\Omega_{\rm F}r^2 - L_{\rm n}\mathcal{M}^2}{1-\mathcal{M}^2}. \quad (40)$$

For our choice of Bernoulli integral $E(\Psi)$ for $\Psi = \Psi_{\rm tot}$,

$$E_{\rm n}(\Psi_{\rm tot}) = w_0 = \frac{c_0^2}{(\Gamma - 1)} \quad (41)$$

and, for expression (28) for non-relativistic enthalpy $w(r)$, the right-hand side of equation (37) vanishes, so that ${\rm d}\Psi/{\rm d}r \to 0$ for $r \to r_{\rm jet}$. Accordingly, due to equation (36), as ${\rm d}\Omega_{\rm F}^2/{\rm d}\Psi \to$ const, the derivative ${\rm d}\mathcal{M}^2/{\rm d}r \to 0$ at the jet boundary as well.

Now expanding the magnetic flux $\Psi(r)$ and Mach number $\mathcal{M}^2(r)$ to second order in $\delta x = x - x_{\rm jet}$, one can find

$$\mathcal{M}^2(x) = \mathcal{M}_0^2\left[1 + A\left(\frac{\delta x}{x_{\rm jet}}\right)^2 + \ldots\right], \quad (42)$$

$$\Psi(x) = \Psi_{\rm tot}\left[1 - B\left(\frac{\delta x}{x_{\rm jet}}\right)^2 + \ldots\right]. \quad (43)$$

Here, $\mathcal{M}_0 = \mathcal{M}(r_{\rm jet})$,

$$A \approx \frac{x_{\rm jet}^6}{\sigma_{\rm M}\mathcal{M}_0^6}\frac{c^2}{c_0^2}, \quad (44)$$

$$B \approx \frac{x_{\rm jet}^4}{\sigma_{\rm M}\mathcal{M}_0^4} \quad (45)$$

and we again use dimensionless scale (35); inequalities (34) were taken into consideration as well. Analysing expressions (44)–(45), we immediately obtain, for the width of the boundary region $\delta r_1 = r_{\rm jet} - r_1$ (see Appendix for elementary derivation),

$$\frac{\delta r_1}{r_{\rm jet}} = \frac{\sigma_{\rm M}^{1/2}M_0^3}{x_{\rm jet}^3}\frac{c_0}{c}, \quad (46)$$

where distance r_1 corresponds to the condition

$$\mathcal{M}^2(r_1)c_{\rm s}^2(r_1) = \Omega_{\rm F}^2(r_1)r_1^2. \quad (47)$$

It is easy to check that condition (47) implies that at distance $r = r_1$ the pressure of the toroidal magnetic field $B_\varphi^2/8\pi$ becomes comparable with external pressure $P_{\rm ext}$. This gives, for the current, $I(r_1) \approx I_{\rm c}$, where

$$I_{\rm c} = (2\pi)^{1/2}\, r_{\rm jet}\, c\, P_{\rm ext}^{1/2}. \quad (48)$$

Thus, it is this domain that corresponds to final current closure in a jet.

As to the poloidal magnetic field, it can be neglected for supersonic flow, $\mathcal{M}^2 \gg 1$. Indeed, using definitions (1), (15) and the first inequality (34), one obtains

$$\frac{B_{\rm p}}{B_\varphi} \approx \frac{\sigma_{\rm M}^{1/2}}{x_{\rm jet}} \ll 1. \quad (49)$$

Accordingly,

$$\frac{v_\varphi}{v_{\rm p}} \approx \frac{\sigma_{\rm M}^{1/2}}{x_{\rm jet}} \ll 1. \quad (50)$$

Downloaded from https://academic.oup.com/mnras/article-abstract/472/4/3971/4094905/On-the-internal-structure-of-relativistic-jets
by MPI Study of Societies user
on 10 October 2017

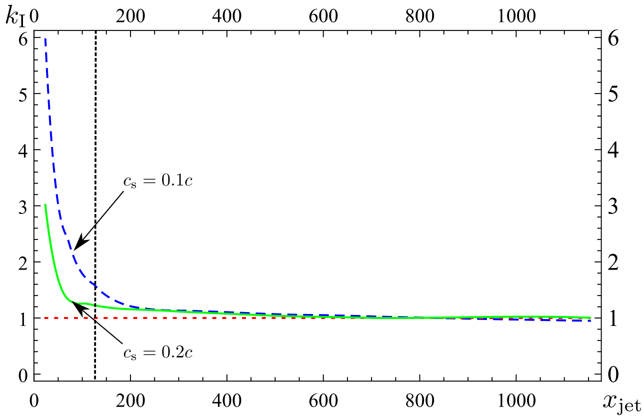

Figure 3. Factor k_{I} for different parameters of a jet. To the left of the vertical line, the right inequality in (34) does not hold.

Finally, equations (42) and (46) result in

$$\mathcal{M}(r_1) \sim \mathcal{M}(r_{\mathrm{jet}}), \tag{51}$$

i.e. the Mach number does not change so fast in this domain. This supports our assumption $\mathcal{M} \approx \mathcal{M}_0$, which was used in derivation (44)–(45).

3.3 Matching procedure and results

For smaller radii up to distance r_2, where $\Omega_{\mathrm{F}} L = \mu\eta$ (and hence, according to (32), $\gamma_{\max}(r_2) \approx 1$), the flow remains non-relativistic, but the first term on the left-hand side of equation (36) becomes the leading one. For this reason, as is shown in Fig. 2, here one can use invariant H (19):

$$H = \frac{\Omega_{\mathrm{F}}(r)\, r^2 \mu\eta}{\mathcal{M}^2(r)} = \mathrm{const.} \tag{52}$$

As, according to (20), in this region $H = I/2\pi$, one can conclude that here $I = k_{\mathrm{I}} I_{\mathrm{c}}$, where $k_{\mathrm{I}} \approx 1$. Exact values of the factor k_{I} can be found by integrating equations (36) and (37) from $r = r_{\mathrm{jet}}$ (see Fig. 3). As we see to the right of the vertical line (where the right inequality in (34) holds), the condition $k_{\mathrm{I}} \approx 1$ is indeed fulfilled with high accuracy.

It is important that the conservation of integral H is valid not only up to radius r_2, where the flow becomes relativistic, but even to radius $r < r_2$, where the flow becomes magnetically dominated ($\mathcal{M}^2 = \Omega_{\mathrm{F}}^2 r^2/c^2$). As a result, one can write for the invariant H, obtained by integrating equations (12), (14) inward from $r = r_{\mathrm{jet}}$ to $r \sim r_2$,

$$H_{\mathrm{in}}(r_{\mathrm{jet}}, P_{\mathrm{ext}}) = k_{\mathrm{I}} (2\pi)^{-1/2} c\, r_{\mathrm{jet}} P_{\mathrm{ext}}^{1/2}. \tag{53}$$

On the other hand, integrating equations (12), (14) outward from $r = 0$ to the same region $r_2 < r < r_1$ and determining the dependence $H_{\mathrm{out}} = H_{\mathrm{out}}(r_{\mathrm{jet}})$ numerically, we can put

$$H_{\mathrm{in}}(r_{\mathrm{jet}}, P_{\mathrm{ext}}) = H_{\mathrm{out}}(r_{\mathrm{jet}}), \tag{54}$$

which implicitly gives us the relation between jet radius r_{jet} and ambient gas pressure P_{ext}.

It is convenient to introduce dimensionless current $h(x) = 2\pi H/I_{\mathrm{GJ}}$:

$$h = \frac{1}{2}\,\frac{\Omega_{\mathrm{F}}}{\Omega_0}\,\frac{x^2}{\sigma_{\mathrm{M}} \mathcal{M}^2}, \tag{55}$$

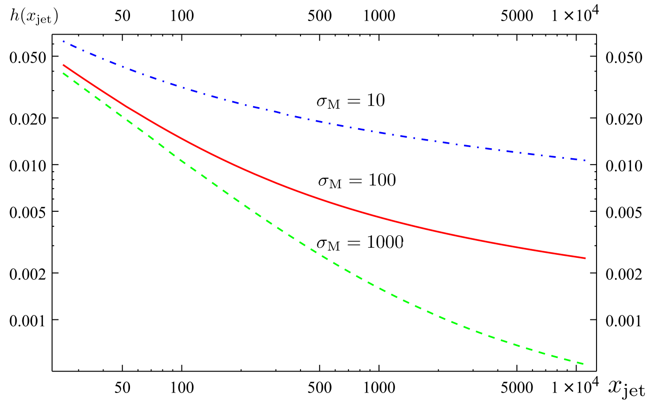

Figure 4. Dimensionless function $h(x_{\mathrm{jet}})$ obtained numerically by solving equation (12), (14) for different magnetization parameters σ_{M}.

where again $x = \Omega_0 r/c$ and

$$I_{\mathrm{GJ}} = \frac{\Omega_0 \Psi_{\mathrm{tot}}}{2\pi} \tag{56}$$

is the total characteristic current corresponding to relativistic Goldreich–Julian charge outflow. Then relation (54) can finally be rewritten as

$$x_{\mathrm{jet}} = \frac{1}{2(2\pi)^{1/2}}\,\frac{h(x_{\mathrm{jet}})}{k_{\mathrm{I}}}\,\frac{B_{\mathrm{L}}}{P_{\mathrm{ext}}^{1/2}}, \tag{57}$$

where again B_{L} (58) is the magnetic field at the light cylinder.

In Fig. 4, we show the dimensionless function $h(x)$ obtained for $\sigma_{\mathrm{M}} = 10$, 10^2 and 10^3. As we see this factor is much smaller than unity. According to its definition $h = I/I_{\mathrm{GJ}}$ in the non-relativistic region $r_2 < r < r_{\mathrm{jet}}$, this implies that the total current returning in the vicinity of the boundary of a jet $r_1 < r < r_{\mathrm{jet}}$ is much smaller than the total current I_{GJ} in a jet.

Finally, to estimate numerically the ambient pressure P_{ext} that is necessary to support the observable jet width, one can rewrite relation (57) as

$$P_{\mathrm{ext}} \approx \frac{h^2(x_{\mathrm{jet}})}{x_{\mathrm{jet}}^2}\,\frac{B_{\mathrm{L}}^2}{8\pi}. \tag{58}$$

As one can check, it is the additional factor $h^2(x_{\mathrm{jet}}) \ll 1$ that differentiates our self-consistent estimation from the standard evaluation corresponding to $I_{\mathrm{GJ}}^2/(2\pi r_{\mathrm{jet}}^2) = P_{\mathrm{ext}}$.

It's necessary to notice that relation $P_{\mathrm{ext}} = B_{\varphi}^2/8\pi = B_{\mathrm{L}}^2/(8\pi x_{\mathrm{jet}}^2)$ was widely used in discussing the equilibrium of the jet (see e.g. Lery et al. 1998; Zakamska et al. 2008; Lyubarsky 2009). However, as we see in reality $I_{\mathrm{c}} \ll I_{\mathrm{GJ}}$ ($h \ll 1$). Accordingly, the value $\Omega_{\mathrm{F}}(r_1)$ is much smaller than the characteristic angular velocity Ω_0. The same concerns the angular momentum L. As a result, toroidal magnetic field $B_{\varphi}(r_1)$ is much smaller that in the main volume of a flow and is to be found self-consistently by solving a general system of equations. It is this point that distinguishes our consideration from most previous ones.

On the other hand, relation (58) gives us the implicit connection between ambient pressure P_{ext} and transverse radius r_{jet}. The advantage of this method is that the matching of relativistic equations occurs not at the jet boundary but in the region where thermal effects are not yet significant.

In Fig. 5, we show how the ambient pressure P_{ext} depends on the transverse dimension of a jet r_{jet} for central mass $M = 10^9\,\mathrm{M}_{\odot}$ (gravitational radius $r_{\mathrm{g}} \sim 3 \times 10^{14}$ cm) and $\Omega_0 r_{\mathrm{g}}/c = 0.1$ and for different magnetization parameters σ_{M}. We also use the

Downloaded from https://academic.oup.com/mnras/article-abstract/472/4/3971/4094905/On-the-internal-structure-of-relativistic-jets
by MPI Study of Societies user
on 10 October 2017

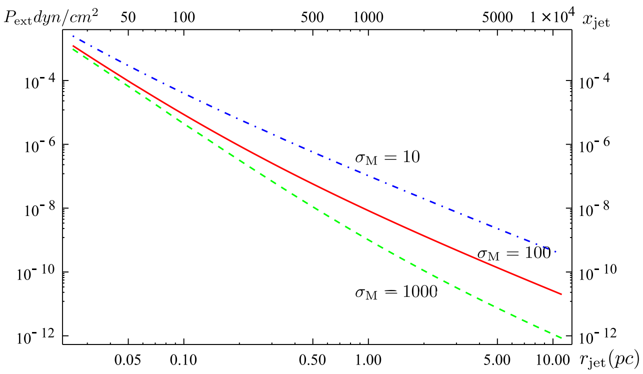

Figure 5. Ambient pressure $P_{\rm ext}$ as a function of jet radius $r_{\rm jet}$ (pc) for different magnetization parameters $\sigma_{\rm M}$.

standard value $B(r_{\rm g}) = 10^4$ G, which gives $B_{\rm L} = 10^2$ G. As we see for parsec-scale jets ($r_{\rm jet} \sim 1$ pc) the ambient pressure should be 10^{-8}–10^{-10} dyne cm^{-2}, which looks rather reasonable for small magnetization of a jet $\sigma_{\rm M} \sim 10$.

There are different estimates of how far from the jet origin the jet radius reaches a size of the order of 1 pc. Thus, the question of a realistic pressure model is open. On the one hand, ambient pressure $P_{\rm ext} \sim 10^{-9}$ dyn cm^{-2} can be expected at a few tens of pc if we consider typical interstellar medium (ISM) values $T_{\rm ism} \sim 1$ keV for the temperature and $n_{\rm e} \sim 1$ cm^{-3} for number density (Krolik 1999; Meier 2012). On the other hand, according to recent observations at distances $l \sim 10$–100 pc from the 'central engine', the collimation of jets is high enough: $\gamma\theta \sim 0.1$–0.2 (Clausen-Brown et al. 2013). Here, θ is the jet half-opening angle. It results in $l \sim 100$ pc for $r_{\rm jet} \sim 1$ pc and $\gamma \sim 10$. On the other hand, the observations presented by Hervet et al. (2017) reveal a typical jet radius of 1 pc at distances 5–10 pc from the jet origin.

4 DISCUSSION AND CONCLUSION

We succeeded in constructing a solution that describes the internal structure of a cylindrical magnetically dominated jet submerged in ambient medium with pure gas pressure. Neither an external magnetic field nor an infinitely thin current sheet or cocoon were assumed. The physical answer depends on the ambient pressure $P_{\rm ext}$ only. Moreover, resolving the current closure region, we determine the thickness of the boundary zone δr_1 (46) (see Appendix for more details).

Also, it was shown that for magnetically dominated jets only a small part $h \ll 1$ (55) of the total current $I \sim I_{\rm GJ}$ is closed in the boundary layer. The greater part of the return current flows in the region $r < r_2$, where the invariant $L(\Psi)$ starts to decrease as a function of Ψ. Of course, the actual dependence (which is determined by the conditions in the central engine) is not known exactly. For this reason, we consider here the model dependence only.

The results are fully applicable not only to a conical jet boundary shape. The method presented of an accurate balance of jet pressure with outer medium pressure is the most general. As has been shown by Nokhrina et al. (2015), the cylindrical approach can be reliably applied for the causally connected parts of relativistic outflows. In particular, all outflows collimated not slower than a parabola are casually connected and may be described by the cylindrical model. As to the conical shape, Zakamska et al. (2008), Komissarov et al. (2009) and Tchekhovskoy et al. (2009) showed that, for small angles described by $\gamma\theta \approx 0.1$, the conical shapes also meet the criteria of casual connectivity across the jet.

A very important conclusion is that the solution inevitably contains a contact discontinuity at the jet boundary. Unlike the electromagnetic discontinuity that has been widely considered thus far, in our solution we deal with a pure hydrodynamical discontinuity. It may be considered as an additional cause of the wave structure of the jet thickness that was detected in recent VLBI observations (Mertens et al. 2016; Pushkarev et al. 2017). Certainly, careful analysis of the appropriate instability is beyond the scope of the present article.

It is also important to stress that, for us, the ambient pressure $P_{\rm ext}$ plays the role of a boundary condition. Its nature is beyond the scope of our consideration. Remember that ambient pressure can be determined not only by the proper temperature of the ambient gas but also by the heating processes resulting from interaction of the supersonic flow of a jet with an external medium (Tchekhovskoy & Bromberg 2016).

Next, we should to point out that, knowing how the jet thickness $r_{\rm jet}(l)$ depends on the distance l from the 'central engine', we have the opportunity to obtain additional information about the ambient pressure $P_{\rm ext}(l)$ dependence on l. Indeed, the last VLBI observations have shown that in most AGN relativistic jets a power-law dependence $r_{\rm jet} \propto l^{\varkappa}$ with $\varkappa = 0.8$–1.2 takes place (Pushkarev et al. 2017). In particular, for jets from M87, observations give $r_{\rm jet} \propto l^{0.6}$ (Asada & Nakamura 2012; Hada 2013; Mertens et al. 2016). On the other hand, as one can see from Fig. 4, for large enough magnetization parameters $\sigma_{\rm M} > 10^3$ (or small enough jet width $x_{\rm jet}$), the dimensionless function $h(x)$ has a power-law dependence as well, i.e. $h(x) \propto x^{-k}$ where $k \approx 0.9$. Using expression (57) for $h(x)$, one can obtain

$$P_{\rm ext}(l) \propto l^{-p}, \tag{59}$$

where $p = 2\varkappa(1 + k) \approx 3$–4.

Finally, as one can see from Fig. 4, for small enough magnetization parameters $\sigma_{\rm M} < 10^3$, for large jet radii $r_{\rm jet}$ the slope $h(x)$ is not so steep. This break connects with different regimes, corresponding to magnetically dominated flow at small distances l from the origin and a saturation regime at larger distances. Indeed, for quasi-cylindrical jets, the following asymptotic solution for magnetically dominated flow exists: $\gamma(r) = r/R_{\rm L}$ (see e.g. Beskin 2009). As, according to Zamaninasab et al. (2014), $R_{\rm L} \approx 10\, r_{\rm g} \sim 10^{14}$ cm, at large enough distances l from the 'central engine', where the transverse dimension of the jet $r_{\rm jet}$ reaches 1 pc so that $r_{\rm jet}/R_{\rm L} > \sigma_{\rm M}$, the flow cannot still be magnetically dominated. Diminishing of the particle acceleration at large distances from the origin was also detected recently by the Monitoring of Jets in Active galactic nuclei with VLBA Experiments (MOJAVE) team (Homan et al. 2015). Some astrophysical applications are considered in Kovalev et al. (personal communication (in preparation)).

ACKNOWLEDGEMENTS

We acknowledge Jonathan Ferreira, Yakov Istomin, Yuri Kovalev, Guy Pelletier and Denis Sobyanin for useful discussions and the anonymous referee for instructive comments, which helped us to improve the manuscript. This work was supported by Russian Science Foundation, grant 16-12-10051.

REFERENCES

Al'pert Y. L., Gurevich A., Pitaevskii L., 1965, Space Physics with Artificial Satellites. Consultants Bureau, New York

Downloaded from https://academic.oup.com/mnras/article-abstract/472/4/3971/4094905/On-the-internal-structure-of-relativistic-jets
by MPI Study of Societies user
on 10 October 2017

Appl S., Camenzind M., 1992, A&A, 256, 354
Appl S., Camenzind M., 1993, A&A, 274, 699
Asada K., Nakamura M., 2012, ApJ, 745, L28
Benford G., Protheroe R. J., 2008a, MNRAS, 382, 663
Benford G., Protheroe R. J., 2008b, MNRAS, 383, 663
Beskin V., 2009, MHD Flows in Compact Astrophysical Objects. Springer-Verlag, Heidelberg
Beskin V., Malyshkin L., 2000, Astron. Lett., 26, 208
Beskin V. S., Nokhrina E. E., 2006, MNRAS, 367, 375
Beskin V. S., Nokhrina E. E., 2010, Astron. Rep., 54, 735
Beskin V. S., Kuznetsova I. V., Rafikov R. R., 1998, MNRAS, 299, 341
Blandford R. D., 1976, MNRAS, 176, 465
Blandford R. D., Payne D. G., 1982, MNRAS, 199, 883
Clausen-Brown E., Savolainen T., Pushkarev A. B., Kovalev Y. Y., Zensus J. A., 2013, A&A, 558, 9
Cohen A. S., Lane W. M., Cotton W. D., Kassim N. E., Lazio T. J. W., Perley R. A., Condon J. J., Erickson W. C., 2007, AJ, 134, 1245
Gracia J., Vlahakis N., Agudo I., Tsinganos K., Bogovalov S. V., 2009, ApJ, 695, 503
Hada K., 2013, in Gómes J. L., ed., Vol. 61, The Innermost Regions of Relativistic Jets and Their Magnetic Fields. EDP Science, Les Ulis
Hervet O., Meliani Z., Zech A., Boisson C., Cayatte V., Sauty C., Sol H., 2017, A&A, in press
Heyvaerts J., Norman C., 1989, ApJ, 347, 1055
Homan D. C., Lister M. L., Kovalev Y. Y., Pushkarev A. B., Savolainen T., Kellermann K. I., Richards J. L., Ros E., 2015, ApJ, 798, 134
Kardashev N. S. et al., 2014, Phys.-Uspekhi, 57, 1199
Kim J., Balsara D. S., Lyutikov M., Komissarov S. S., 2016, MNRAS, 461, 728
Kim J., Balsara D. S., Lyutikov M., Komissarov S. S., 2017, MNRAS, 467, 4647
Koide S., Shibata K., Kudoh T., 1999, ApJ, 522, 727
Komissarov S. S., Barkov M. V., Vlahakis N., Königl A., 2007, MNRAS, 380, 51
Komissarov S. S., Vlahakis N., Knigl A., Barkov M. V., 2009, MNRAS, 394, 1182
Krolik J. H., 1999, Active galactic nuclei : from the central black hole to the galactic environment. Princeton Univ. Press, Princeton NJ
Lery T., Heyvaerts J., Appl S., Norman C. A., 1998, A&A, 337, 603
Lesch H., Appl S., Camenzind M., 1989, A&A, 225, 341
Lico R., Gómez J. L., Asada K., Fuentes A., 2007, MNRAS, 469, 1612
Li Z.-Y., Chiueh T., Begelman M. C., 1992, ApJ, 394, 459
Lobanov A. P., 1998a, A&A, 132, 261
Lobanov A. P., 1998b, A&A, 330, 79
Lovelace R. V. E., 1976, Nature, 262, 649
Lynden-Bell D., 1996, MNRAS, 279, 389
Lynden-Bell D., 2003, MNRAS, 341, 1360
Lyubarsky Y., 2009, ApJ, 698, 1570
McKinney J. C., 2006, MNRAS, 368, 1561
McKinney J. C., Tchekhovskoy A., Blandford R. D., 2012, MNRAS, 423, 3083
Meier D. L., 2012, Black Hole Astrophysics the Engine Paradigm. Springer-Verlag, Berlin
Mertens F., Lobanov A. P., Walker R. C., Hardee P. E., 2016, A&A, 595, 20
Michel F. C., 1969, ApJ, 158, 727
Mizuno Y., Lyubarsky Y., Nishikawa K.-I., Hardee P. E., 2012, ApJ, 757, 12
Mościbrodzka M., Falcke H., Shiokawa H., 2016, A&A, 586, 15
Nokhrina E., Beskin V., Kovalev Y., Zheltoukhov A., 2015, MNRAS, 447, 2726
Pelletier G., Pudritz R. E., 1992, ApJ, 394, 117
Penna R. F., Narayan R., Sądowski A., 2013, MNRAS, 436, 3741
Porth O., Fendt C., Meliani Z., Vaidya B., 2011, ApJ, 737, 42
Pushkarev A. B., Kovalev Y. Y., Lister M. L., Savolainen T., 2017, MNRAS, 468, 4992
Sauty C., Tsinganos K., 1994, A&A, 287, 893
Sulkanen M. E., Lovelace R. V. E., 1990, ApJ, 350, 732
Tchekhovskoy A., Bromberg O., 2016, MNRAS, 461, L46
Tchekhovskoy A., McKinney J. C., Narayan R., 2009, ApJ, 699, 1789
Tomimatsu A., 1994, PASJ, 46, 123
Tomimatsu A., Takahashi M., 2003, ApJ, 592, 321
Weber E. J., Davis L. J., 1967, ApJ, 148, 217
Zakamska N. L., Begelman M. C., Blandford R. D., 2008, ApJ, 679, 990
Zamaninasab M., Clausen-Brown E., Savolainen T., Tchekhovskoy A., 2014, Nature, 510, 126
Zheleznyakov V., 1996, Radiation in Astrophysical Plasmas. Springer-Verlag, Heidelberg

APPENDIX: CURRENT CLOSURE WIDTH

In this Appendix, we show how expression (46) for the current closure width δr_1 can be obtained from elementary considerations. In the supersonic regime, the force balance equation for $r \approx r_{\rm jet}$ can be written as

$$\frac{\mathrm{d}}{\mathrm{d}r}\left(\frac{B_\varphi^2}{8\pi} + P\right) = 0. \tag{A1}$$

As one can easily check, this condition corresponds exactly to the following terms in equation (36):

$$c_{\rm s}^2 \frac{\mathrm{d}\mathcal{M}^2}{\mathrm{d}r} = \frac{1}{2} r^2 \frac{\mathrm{d}\Psi}{\mathrm{d}r}\frac{\mathrm{d}\Omega_{\rm F}^2}{\mathrm{d}\Psi}. \tag{A2}$$

On the other hand, as was shown above, the characteristic scale of changing $\mathcal{M}^2$ (and hence the pressure P) is similar to the width δr_1. This allows us to write

$$\frac{\mathrm{d}P}{\mathrm{d}r} \approx \frac{P_{\rm ext}}{(\delta r_1)^2}\, x, \tag{A3}$$

where $x = r_{\rm jet} - r$. Now using definition (1) for B_φ and the supersonic asymptotic solution

$$I = \frac{2\pi c \eta_{\rm n} \Omega_{\rm F} r_{\rm jet}^2}{\mathcal{M}_0^2} \tag{A4}$$

for current I, we obtain

$$\left(\frac{\delta r_1}{r_{\rm jet}}\right)^2 \approx \frac{P_{\rm ext}\mathcal{M}_0^4}{2\pi r_{\rm jet}^4 \eta_{\rm n}^2 (\Omega')^2}, \tag{A5}$$

where $\Omega' = \mathrm{d}\Omega_{\rm F}/\mathrm{d}r$ for $r = r_{\rm jet}$. Additionally, the definition (22) for $\Omega_{\rm F}$ results in

$$(\Omega')^2 = \pi \frac{\Omega_0^2 r_{\rm jet}}{\Psi_{\rm tot}}\, B_{\rm p}'. \tag{A6}$$

Now using the leading terms of the Bernoulli equation,

$$\frac{v^2}{2} \approx \Omega_{\rm F} L_{\rm n}, \tag{A7}$$

the connection $\rho_{\rm ext} v' = \eta_{\rm n} B_{\rm p}'$ resulting from definition (3), where again the primes denote the appropriate derivatives, and also the clear expression for magnetic flux,

$$\Psi \approx \Psi_{\rm tot} - \pi r_{\rm jet} B_{\rm p}' x^2, \tag{A8}$$

and definition (21) for $L(\Psi)$, we finally obtain

$$B_{\rm p}' \approx \frac{1}{2\pi}\,\frac{\Omega_0^2}{c\eta_{\rm n}^3}\, r_{\rm jet}\rho_{\rm ext}^2. \tag{A9}$$

Together with (A5) and (A6), this gives us the expression (46) for δr_1.

This paper has been typeset from a TEX/LATEX file prepared by the author.

Downloaded from https://academic.oup.com/mnras/article-abstract/472/4/3971/4094905/On-the-internal-structure-of-relativistic-jets
by MPI Study of Societies user
on 10 October 2017